Mutant superoxide dismutase 1-induced IL-1β accelerates ALS pathogenesis

Felix Meissner[1], Kaaweh Molawi[1], and Arturo Zychlinsky[2]

Department of Cellular Microbiology, Max Planck Institute for Infection Biology, 10117 Berlin, Germany

Edited* by Charles A. Dinarello, University of Colorado, Aurora, CO, and approved June 2, 2010 (received for review February 26, 2010)

ALS is a fatal motor neuron disease of adult onset. Neuroinflammation contributes to ALS disease progression; however, the inflammatory trigger remains unclear. We report that ALS–linked mutant superoxide dismutase 1 (SOD1) activates caspase-1 and IL-1β in microglia. Cytoplasmic accumulation of mutant SOD1 was sensed by an ASC containing inflammasome and antagonized by autophagy, limiting caspase-1–mediated inflammation. Notably, mutant SOD1 induced IL-1β correlated with amyloid-like misfolding and was independent of dismutase activity. Deficiency in caspase-1 or IL-1β or treatment with recombinant IL-1 receptor antagonist (IL-1RA) extended the lifespan of G93A-*SOD1* transgenic mice and attenuated inflammatory pathology. These findings identify microglial IL-1β as a causative event of neuroinflammation and suggest IL-1 as a potential therapeutic target in ALS.

caspase-1 | inflammasome | interleukin 1 | Lou Gehrig's disease | neurodegeneration

ALS is a fatal neurodegenerative disorder characterized by progressive loss of motor neurons causing paralysis and finally death within 1–5 years after diagnosis. Dominant gain of function mutations of SOD1 are the most common genetic cause of ALS and also lead to motor neuron disease in mutant *SOD1* transgenic mice (1). Mutations induce toxic misfolding and aggregation of SOD1 and interfere with cellular homeostasis in neurons and glia cells (2, 3). Neurodegeneration in ALS is accompanied by glia mediated neuroinflammation, which accelerates disease progression non–cell-autonomously (2, 4). One of the inflammatory markers found in the CNS of ALS mice is active caspase-1, which is also implicated in amyloid-β–mediated inflammation (5–7). Caspase-1 is activated in response to danger signals by cytosolic protein complexes called inflammasomes and proteolytically matures IL-1β and IL-18 (8). Accordingly, IL-1β levels are elevated in the CNS of mutant *SOD1* transgenic mice and ALS patients (7). Extracellular mutant SOD1 has been shown to induce an inflammatory reaction by microglia (9, 10); however, the underlying mechanisms are poorly understood.

Results

Mutant SOD1 Activates Caspase-1 in Microglia. To test whether mutant SOD1 can act as a danger signal that activates caspase-1 in resident microglia, we stimulated these cells with purified WT or mutant G93A-SOD1. G93A-SOD1, but not the WT protein, activated caspase-1 in microglia and macrophages in a dose-dependent manner (Fig. 1 *A* and *B*). Consistently, time- and dose-dependent secretion of mature IL-1β was observed specifically upon G93A-SOD1 stimulation of microglia or macrophages (Figs. 1*C* and S1). G93A-SOD1 induced IL-1β maturation was dependent on caspase-1 and could not be observed in astrocytes (Fig. 1 *D* and *E*). Notably, caspase-1–mediated IL-1β release in response to G93A-SOD1 was independent of nonproteinaceous contaminants, LPS priming or transgenic mutant SOD1 expression in microglia or macrophages (Figs. S2 and S3). The inflammasome adaptor protein apoptosis-associated speck-like protein containing a caspase recruitment domain (ASC) was essential for IL-1β release in response to G93A-SOD1, whereas the Nod-like receptors (NLRs) NALP3 and IPAF were not required (Fig. S4). Collectively, these data demonstrate that mutant G93A-SOD1 activates caspase-1 and induces IL-1β maturation in microglia and macrophages in an ASC-dependent manner.

Autophagy Counteracts Cytoplasmic SOD1 Accumulation and Caspase-1 Activation. Further analysis of the mechanism of caspase-1 activation by mutant SOD1 revealed rapid endocytosis of fluorescently labeled SOD1 (Fig. 2 *A* and *B*). This could be blocked by cytochalasin D, an inhibitor of actin polymerization, which also inhibited mutant SOD1–induced IL-1β release, indicating that uptake of mutant SOD1 is required for caspase-1 activation (Fig. 2*C*).

Because several caspase-1 activators require endocytosis and translocate into the cytoplasm, we next analyzed the subcellular distribution of SOD1 by differential subcellular extraction (5, 11). Biochemical analysis of the cytosol and the organelle fraction of SOD1 stimulated macrophages showed that SOD1 partially relocated from the organelle fraction into the cytoplasm within 5 min where it accumulated at later time points (Fig. 2*D*). Confocal microscopy of macrophages coincubated with fluorophore-labeled mutant SOD1 and fluorescent dextran, which traffics into the endo-lysosomal pathway, support these results (Fig. 2*E*). Notably, mutant SOD1 is taken up more efficiently than WT SOD1, resulting in increased cytoplasmic accumulation of the mutant protein (Fig. S5).

We speculated that cytoplasmic accumulation of SOD1 induces autophagy, a homeostatic cellular process evolved to degrade long-lived cytosolic proteins and macromolecules (12). Pharmacological inhibition of autophagy increased the amount of SOD1 in the cytosolic fraction and strongly increased IL-1β release upon mutant SOD1 stimulation (Fig. 3 *A* and *B*). Notably, WT SOD1-induced IL-1β release was comparable to cells primed only with LPS (13). Furthermore, deficiency in autophagy-related 5 (ATG5), a protein required for autophagosome formation (14), increased caspase-1 activation in response to G93A-SOD1, indicating that autophagosomes were formed as a cellular stress response to remove cytoplasmic SOD1 and to reduce inflammation (Fig. 3*C*).

These data collectively show that endocytosed mutant SOD1 enters the cytoplasm and activates caspase-1, whereas autophagy counteracts cytoplasmic SOD1 accumulation to dampen the proinflammatory response.

Amyloid Conformation Correlates with IL-1β Maturation. Mutations prompt SOD1 to misfold into amyloid-like structures in vitro and in vivo (3). To test whether mutation-induced structural changes are involved in caspase-1 activation by mutant SOD1, we analyzed WT-SOD1 and three well-studied SOD1 mutants (G93A, G85R,

Author contributions: F.M., K.M., and A.Z. designed research; F.M. and K.M. performed research; F.M., K.M., and A.Z. analyzed data; and F.M., K.M., and A.Z. wrote the paper.

The authors declare no conflict of interest.

*This Direct Submission article had a prearranged editor.

See Commentary on page 12741.

[1]F.M. and K.M. contributed equally to this work.

[2]To whom correspondence should be addressed. E-mail: zychlinsky@mpiib-berlin.mpg.de.

This article contains supporting information online at www.pnas.org/lookup/suppl/doi:10.1073/pnas.1002396107/-/DCSupplemental.

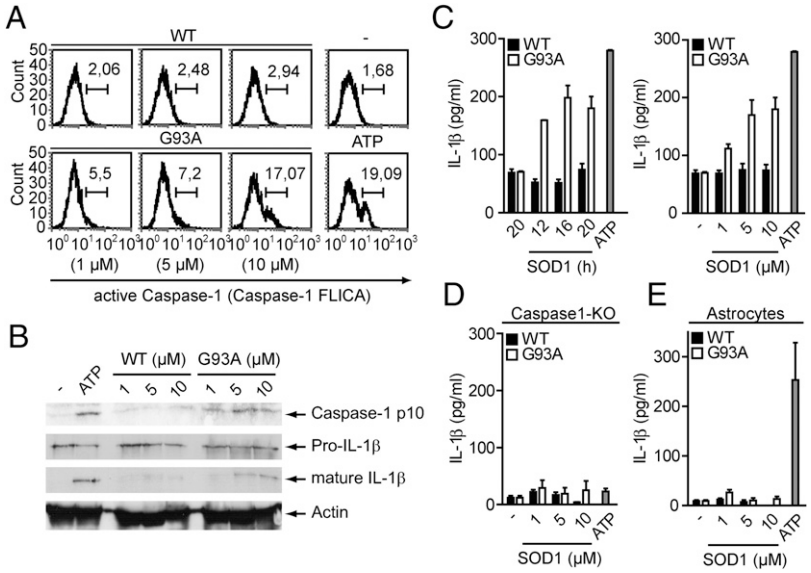

Fig. 1. Mutant SOD1 activates caspase-1 in microglia and macrophages. (*A–E*) Primed cells were stimulated with 10 μM or the depicted concentrations of WT or G93A-SOD1 for 20 h or as indicated. (*A*) Flow cytometry analysis of caspase-1 activation in primary microglia by a fluorescent cell-permeable inhibitor that binds to active caspase-1 (FLICA). Numbers above bracketed lines indicate percentage of cells with active caspase-1. Unstimulated and ATP-stimulated cells served as controls. (*B*) Immunoblot analysis of cell lysates and supernatants of stimulated bone marrow–derived macrophages (BMMs) with antibodies to the p10 subunit of caspase-1 and to IL-1β, respectively. Actin shows equal loading of lanes. (*C–E*) ELISA analysis of secreted, mature IL-1β in the cell supernatant of stimulated primary microglia (*C*), caspase-1–deficient BMMs (*D*), or primary astrocytes (*E*). Data are representative of at least three independent experiments; error bars represent SEM of triplicate wells.

and G37R) for their propensity to form amyloids using Thioflavin-T (Th-T) fluorescence. All three mutant SOD1 proteins showed a remarkable increase in Th-T fluorescence compared with the WT protein (Fig. S6*A*). G93A-SOD1, which exhibited the highest Th-T fluorescence, potently activated caspase-1 and IL-1β secretion; G37R- and G85R-SOD1 mutants, with intermediate amyloid characteristics, were weaker caspase-1 and IL-1β activators than G93A-SOD1 (Fig. S6 *B* and *C*), suggesting a connection between these two parameters. Interestingly, when we tested nine different SOD1 mutants and the WT protein, we observed a significant, direct correlation between the Th-T fluorescence and the secretion of mature IL-1β (Fig. 4 *A–C*).

Furthermore, caspase-1 activation was not dependent on the superoxide degrading activity of SOD1. The metalloprotein SOD1 was enzymatically inactive when purified and tested in the absence of copper and zinc (Fig. S6*D*). Metalation restored SOD1 activity, which was equally high in WT and G93A-SOD1, intermediate in G37R-SOD1, and poor in G85R-SOD1. However, metalation did not affect caspase-1 activation nor influence Th-T binding in any of the SOD1 proteins tested (Fig. S6 *E* and *F*). Together, these results suggest that mutant SOD1 induces caspase-1 activation independently of its enzymatic activity through a gain of amyloid conformation.

IL-1β Promotes Disease Progression in G93A-SOD1 Mice. To determine the contribution of caspase-1 and caspase-1–dependent cytokines to motor neuron disease in vivo, we crossed G93A-*SOD1* transgenic mice (15) with caspase-1–, IL-1β– or IL-18–deficient mice and monitored survival. Deficiency in caspase-1 or IL-1β equally extended the lifespan of G93A-*SOD1* transgenic animals, whereas deficiency in IL-18 did not affect survival (Fig. 5*A*). Disease onset remained unchanged in IL-1β–deficient G93A-*SOD1* transgenic mice (Fig. S7). Immunohistochemical analysis revealed reduced microgliosis and astrogliosis coinciding with an increased number of motor neurons in the spinal cord of caspase-1– and IL-1β–deficient G93A-*SOD1* transgenic mice in comparison with controls (Fig. 5 *B–D*). These findings suggested IL-1β as a therapeutic target to slow down disease progression in G93A-*SOD1* transgenic mice. IL-1 bioactivity is controlled by the highly specific endogenous interleukin-1 receptor antagonist (IL-1RA) (16). Treatment of transgenic mice with recombinant human IL-1RA (Anakinra) significantly extended survival and improved motor function during the symptomatic phase in comparison with placebo-treated controls (Fig. 5 *E* and *F*).

These data demonstrate that IL-1β contributes significantly to disease progression in G93A-*SOD1* transgenic animals by promoting neuroinflammation. Inhibition of IL-1 signaling by IL-1RA treatment represents a potential medical intervention in ALS, as it prolonged the lifespan of G93A-*SOD1* transgenic animals.

Discussion

Motor neuron degeneration in ALS is accompanied by inflammation, which involves microgliosis and astrogliosis as well as the up-regulation of proinflammatory molecules in the CNS (4, 17, 18). Here we identified misfolded mutant SOD1 as a disease-associated endogenous danger signal that is sensed by microglia and initiates inflammation through caspase-1–dependent IL-1β maturation. Mutant SOD1 has been described to form amyloid-like oligomers and aggregates in vitro and in vivo (3, 19–21). We demonstrate that the degree of amyloid-like misfolding of mutant SOD1 correlated with IL-1β maturation, supporting the recent finding that SOD1 aggregate formation is linked to accelerated disease progression in ALS patients (22). Notably, mutant SOD1-induced inflammasome activation was independent of LPS priming and the NLRs NALP3 and IPAF. These observations raise the possibility that mutant SOD1 is sensed by one or multiple innate immune receptors that also account for the priming, analogously to the recognition of amyloid-β by an inflammasome and TLRs (5, 23, 24).

We showed that mutant SOD1 was efficiently endocytosed and leaked into the cytoplasm to activate caspase-1. Future studies should address whether the increased uptake of mutant SOD1 is a result of a specific cell surface receptor interaction, which might contribute to the innate immune sensing of misfolded proteins such as mutant SOD1. Autophagy antagonized cytoplasmic accumulation of misfolded SOD1 and therefore limited

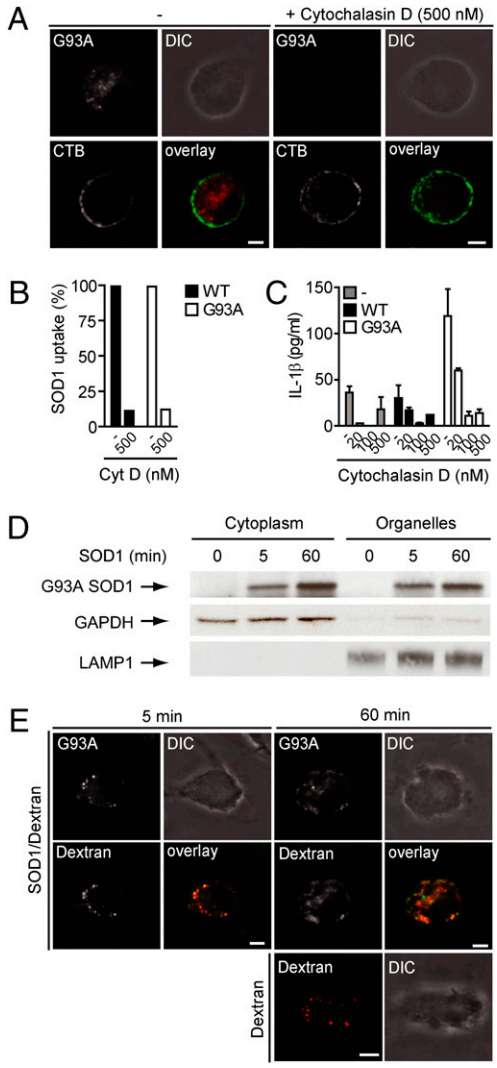

Fig. 2. IL-1β maturation requires endocytosis of mutant SOD1. (*A–D*) Primed BMMs were stimulated with WT or G93A-SOD1 as indicated. (*A* and *B*) Uptake of fluorescently labeled G93A-SOD1 (5 μM; red) in the presence of Cytochalasin D analyzed by confocal microscopy (*A*) or flow cytometry (*B*). Fluorescent cholera toxin B (CTB; green) stains cell membranes. (*C*) ELISA of SOD1 (10 μM) induced mature IL-1β in the presence of Cytochalasin D. (*D*) Immunoblot analysis of cytoplasmic and organelle fraction of BMMs stimulated with G93A-SOD1 (2 μM) for indicated times using antibodies against human SOD1, GAPDH (cytoplasmic marker protein), and LAMP1 (organelle marker protein). (*E*) Confocal microscopy of BMMs stimulated for the indicated time points with labeled G93A-SOD1 (5 mM; green) and Dextran (red) or Dextran only. (Scale bars, 4 μm.) Data are representative of at least three independent experiments; error bars represent SEM of triplicate wells.

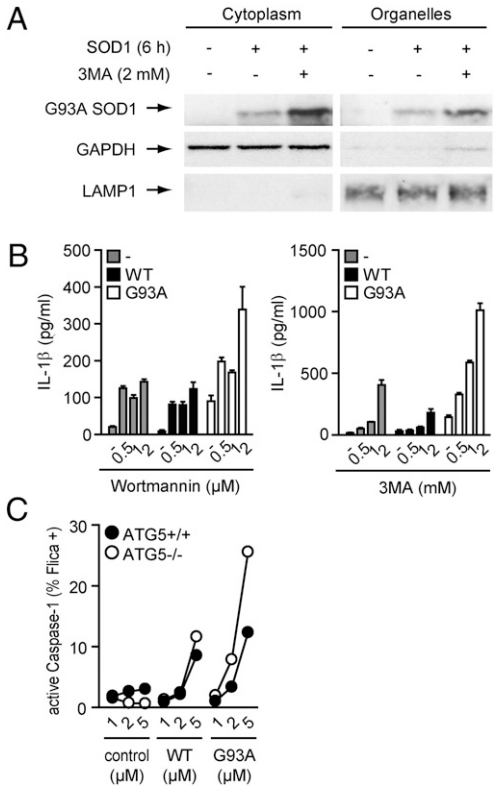

Fig. 3. Mutant SOD1–induced caspase-1 activation is counteracted by autophagy. (*A–C*) Primed cells were stimulated with WT or G93A-SOD1 as indicated. (*A*) Immunoblot analysis of cytoplasmic and organelle fraction of BMMs stimulated with G93A-SOD1 (2 μM) for 6 h in the presence of 3-methyladenine (3MA) using antibodies against human SOD1, GAPDH (cytoplasmic marker protein), and LAMP1 (organelle marker protein). (*B*) ELISA of SOD1 (10 μM) induced mature IL-1β from BMMs in the presence of wortmannin or 3-methyladenine. (*C*) Caspase-1 activation determined by flow cytometry analysis with caspase-1 FLICA in autophagy-related 5–deficient ($ATG5^{-/-}$, ○) and nondeficient $ATG5^{+/+}$ (●) mouse embryonic fibroblasts (MEFs) transfected with the indicated concentrations of SOD1. Data are representative of three independent experiments; error bars represent SEM of triplicate wells.

caspase-1–mediated inflammation, confirming a beneficial function of autophagy in ALS (13).

In G93A-*SOD1* ALS mice, caspase-1 acts through IL-1β, as caspase-1– and IL-1β–deficient transgenic mice displayed equal survival extensions. Treatment of ALS mice with IL-1RA further confirmed the relevance of IL-1–mediated inflammation, indicating that caspase-1–induced neuronal cell death described elsewhere seems to play a minor role in this disease model (7). Previous results suggesting that IL-1β does not affect ALS pathogenesis in G37R transgenic ALS mice might be due to the different aggregation and inflammatory properties of the SOD1 mutation (G93A vs. G37R) or to the different mouse strains used (congenic C57BL/6 vs. mixed background B10RIII × C57BL/6) (17). In our experiments, IL-1β deficiency slowed disease progression but did not affect disease onset, arguing for a non–cell-autonomous, microglia-mediated acceleration of neurodegeneration (25). IL-1 is a pleiotropic cytokine involved in the induction of inflammatory and neurotoxic molecules such as COX2, inducible NOS, NO, or IL-6, which are implicated in ALS (4, 16, 18, 26). Therefore our data and the previous finding of active caspase-1 before disease onset suggest IL-1β as an initiating signal of neuroinflammation in ALS (6, 27). It is tempting to speculate that the results presented here not only identified IL-1 as a potential therapeutic target in ALS but also have implications on other conformational diseases involving inflammation.

Methods

Mice. $CASP1^{-/-}$, $IL1\beta^{-/-}$, $IL18^{-/-}$, $IL18/IL1\beta^{-/-}$, and $TLR4^{-/-}$ mice have been described previously (4, 16). TgSOD1-G93A mice on a C57BL/6 background were kindly provided by Albert Ludolph (University of Ulm, Ulm, Germany) (15). TgSOD1-G93A/$CASP1^{-/-}$, TgSOD1-G93A/$IL1\beta^{-/-}$, TgSOD1-G93A/$IL18^{-/-}$, and TgSOD1-G93A/$IL18/IL1\beta^{-/-}$ mice were generated as F2 litters from interbreeding of TgSOD1-G93A and the corresponding knockout mice. The number of SOD1 transgenes was controlled semiquantitatively by real-time PCR as described elsewhere (28). Mice were tested weekly for neuromuscular dysfunction with the hanging-wire test. Latency to fall (maximum 3 min) was measured after a mouse was placed on the bars and turned upside down (height 20 cm). Mice that fell in <10 s were given a second trial. For IL-1RA treatment, SOD1 transgenic animals were injected every 24 h intraperitoneally with either 150 mg/kg or 75 mg/kg IL-1RA in 200 μL NaCl

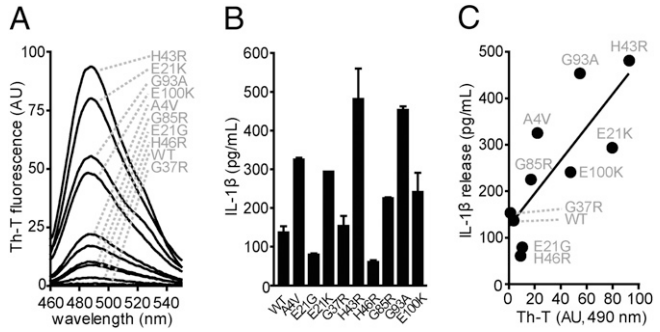

Fig. 4. SOD1-induced IL-1β maturation correlates with its amyloid-like misfolding. (*A*) Th-T fluorescence of the indicated SOD1 proteins. (*B*) IL-1β maturation induced by the indicated SOD1 proteins in primed BMMs determined by ELISA. (*C*) Correlation of IL-1β maturation and its corresponding Th-T fluorescence at 490 nm. $P = 0.0052$; Pearson´s correlation coefficient $r = 0.8027$. AU, arbitrary units. Data are representative of two independent experiments.

solution starting at the age of 70 d. For the placebo group, 200 μL NaCl solution was used for injection. All mice were housed in the Institute's pathogen-free facility. Animal studies were approved by the Landesamt für Gesundheit und Soziales Berlin.

Tissue Culture. Murine microglia and astrocytes were isolated from neonatal brains. Neonatal mouse brains were dissected free of meninges and blood vessels. Minced brains were dissociated with trypsin in HBSS and filtered with 200-μm pore size. A mixed glial culture was prepared by maintaining cells in complete medium containing penicillin/streptomycin in poly-D-lysine–coated flasks for 2 wk. A microglial culture was obtained from the mixed glial culture by shaking flasks for 1 h at 200 rpm in an orbital shaker and allowing the transferred dislodged cells to adhere to new tissue culture dishes. An astrocyte culture was obtained from a trypsinized and detached mixed glial culture by depletion of CD11b–positive cells using MACS (130-093-634, Miltenyi) and replating on new tissue culture dishes. Purity of the microglia and astrocyte culture was analyzed by FACS using antibodies against CD11b and GFAP respectively. Bone marrow–derived macrophages (BMMs) were collected from the femur and tibia of mice. Bone marrow cells were plated on sterile Petri dishes and incubated in DMEM containing 10% FCS, 5% equine serum, 10 mM Hepes, 1 mM pyruvate, 10 mM L-glutamine, and 20% M-CSF–conditioned medium. M-CSF–conditioned medium was collected from an L929 M-CSF cell line. Bone marrow cells were incubated at 37 °C and 7% CO_2, and macrophages were harvested after 6 d. Bone marrow deficient in NALP3, ASC, and IPAF was kindly provided by Eicke Latz (University of Massachusetts Medical School, Worcester, MA) and Vishva Dixit (Genentech, San Francisco). ATG5$^{-/-}$ and ATG5$^{+/+}$ mouse embryonic fibroblasts (MEF) were kindly provided by Noboru Mizushima (Tokyo Medical and Dental University, Tokyo) and grown in DMEM medium supplemented with 10% FCS at 37 °C in 5% CO_2.

Caspase-1 Activity Assays. Cells were primed for 2 h with LPS (100 ng/mL) if indicated. Primary microglia or macrophages were stimulated with WT or mutant SOD1 protein. Unstimulated, ATP stimulated or *Shigella flexneri* (M90T)–infected cells served as controls. MEFs were transfected with purified SOD1 using DOTAP (Roche) according to the manufacturer's instructions. Caspase-1 activation was analyzed in cell lysates by immunoblot or with a fluorescent inhibitor of active caspase-1 (FAM-YVAD-FMK, Immunochemistry Technologies) by FACS (exitation at 488 nm, emission at 515–545 nm). Maturation of the caspase-1 substrate IL-1β was measured in cell supernatants by ELISA from BD or by immunoblot.

Immunoblot. Cells were lysed in buffer containing 1% Nonidet-P40 supplemented with complete protease inhibitor "mixture" (Roche). The protein concentration was measured with BCA Protein Assay Reagent (Pierce), and lysates were adjusted accordingly. For cell fractionation experiments, cellular subfractions were obtained using ProteoExtract Subcellular Proteome Extraction Kit (Calbiochem) according to the manufacturer's instructions. Lysates were boiled 5 min with SDS sample buffer under reducing conditions, resolved by SDS/PAGE, and transferred to nitrocellulose membranes by electroblotting. Samples were incubated for 4 h at 4 °C with the appropriate antibody and analyzed by immunoblot.

Immunohistochemistry. Tissue from 120-d-old mice was fixed by transcardiac perfusion with 4% paraformaldehyde in phosphate buffer. Coronal cryosectioning of the cervical spinal cord was performed at a thickness of 35 μm per section. Every 12th section was stained for microglia or astrocytes using

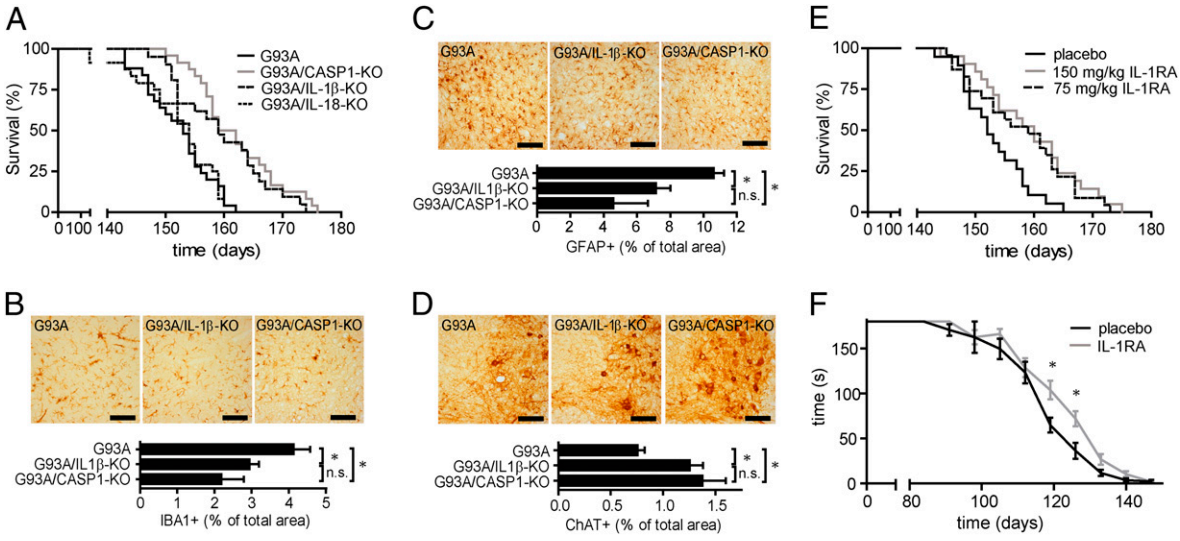

Fig. 5. Disease progression in G93A-*SOD1* transgenic mice is accelerated by IL-1β and can be delayed by IL-1RA treatment. (*A*) Survival of G93A-*SOD1* transgenic mice (152.2 ± 1.2 d; $n = 25$), caspase-1–deficient (162.0 ± 1.8 d; $n = 24$), IL-1β–deficient (159.6 ± 1.7 d; $n = 21$), and IL-18–deficient (152.2 ± 1.4 ds; $n = 24$) G93A-*SOD1* transgenic mice. Caspase-1– and IL-1β–deficient mice lived significantly longer than G93A-*SOD1* transgenic mice ($P < 0.001$). (*B–D*) Immunohistochemical analysis of cervical spinal cord sections of 120-d-old G93A-*SOD1* transgenic mice, caspase-1–deficient G93A-*SOD1* transgenic mice, and IL-1β–deficient G93A-*SOD1* transgenic mice using antibodies against the microglial marker protein ionized calcium binding adaptor molecule 1 (IBA1; *B*), the astrocytic marker glial fibrillary acidic protein (GFAP; *C*), or the motor neuron marker protein choline acetyltransferase (ChAT; *D*). Representative images of the ventral horn area of mice with indicated genotypes, and quantification of IBA1-, GFAP-, and ChAT-positive area in the ventral horns of analyzed mice. (*E*) Survival of G93A-*SOD1* transgenic mice treated with indicated dosages of IL-1RA (75 mg/kg: 157.8 ± 1.8 d, $n = 23$; 150 mg/kg: 159.4 ± 1.8 d; $n = 21$) or placebo (153.1 ± 1.3 d, $n = 19$). IL-1RA–treated mice lived significantly longer than placebo-injected mice (75 mg/kg, $P = 0.0145$; 150 mg/kg, $P < 0.005$). (*F*) Motor performance of IL-1RA (150 mg/kg) and placebo-treated G93A-*SOD1* transgenic mice determined by the hanging-wire test. (Scale bar, 200 μm.) $^*P < 0.05$. n.s, Not significant. Values are mean ± SEM.

antibodies against IBA1 (1:15,000; WAKO), GFAP (1:20,000; DAKO) or ChAT (1:1,000; Chemicon) respectively. Immunoreactivity was visualized with diaminobenzidine (DAB; Vectastain elite ABC kit, Vectorlabs). Anterior horn area of every 12th section was photographed (Zeiss Axioplan microscope), and DAB-positive area was quantified using ImageJ software (National Institutes of Health). A minimum of eight sections per mouse were analyzed. Each group contained at least four mice.

Immunofluorescence. For immunofluorescence, cells were seeded on coverslips and stimulated with WT or mutant SOD1 conjugated with ATTO-488 or Cy-5. To follow endocytosis and subcellular distribution upon SOD1 uptake, cells were coincubated with Alexa Fluor 647–conjugated dextran as described elsewhere (11). At defined time points, cells were rinsed with PBS, fixed with PFA, and permeabilized with 0.1% Triton X-100. All antibodies were diluted in PBS + 0.5% BSA according to the manufacturer's instructions. Coverslips were mounted on microscope slides and analyzed using a confocal fluorescence microscope (TCS SP, Leica).

Flow Cytometry. At least 5,000 cells were acquired and analyzed by flow cytometry using a FACSCalibur flow cytometer (BD Biosciences). Data were analyzed and processed by FCS Express version 3 (De Novo Software).

Thioflavin-T Fluorescence. Measurements were taken in a LS55 fluorescence spectrophotometer (Perkin-Elmer) using a 1-cm path-length glass cell. A 20-μg quantity of SOD1 was incubated in 1 mL of 5 μM of Th-T in 50 mM glycine/NaOH, pH 8.2. Excitation was at 446 nm and emission was recorded from 460 to 600 nm at 1-nm intervals. Scans were done in triplicate per sample. Appropriate blank spectra were recorded on buffer components and subtracted from spectra obtained on protein samples.

Expression and Purification of SOD1. Human SOD1 cDNA sequences (WT, A4V, E21G, E21K, G37R, H43R, H46R, G85R, G93A, and E100K) were cloned into pGEX-6P-1 *Escherichia coli* expression vector (GE Healthcare). After induction by 0.5 mM isopropyl-1-thio-s-D-galactopyranoside (IPTG) for 1 h at 30 °C in *E. coli* (BL21 RIL), cells were lysed and centrifuged at 10,000 × *g*. GST-SOD1 was cleared from the supernatant with GSH-Sepharose (Sigma), and SOD1 was released from Sepharose by cleavage with PreScission Protease (GE Healthcare). SOD1 was subjected to gel filtration chromatography on a Superdex 75 column (GE Healthcare) and was stored in 20 mM Hepes (pH 7.4), 50 mM NaCl, and 1 mM DTT. EndoTrap Red endotoxin removal system (Profos) was used in case further purification was necessary.

Statistical Analysis. Data were analyzed with the two-tailed Student's *t* test. Survival rates were analyzed by the Kaplan–Meier method and were compared by the log-rank test. Correlation was analyzed using linear regression and Pearson's correlation coefficient.

ACKNOWLEDGMENTS. We thank Eicke Latz (University of Massachusetts), Vishva Dixit (Genentech), and Noboru Mizushima (Tokyo Medical and Dental University) for generously providing knockout cells; the members of the Zychlinsky laboratory for advice and discussion, especially Juana de Diego, Anna Brotcke, and Venizelos Papayannopoulos; and Steven Dewitz, Robert Hurwitz, Britta Laube, Jutta Lambers, Yvonne Uhlemann, Jens Otto, and the animal caretakers for technical assistance.

1. Rothstein JD (2009) Current hypotheses for the underlying biology of amyotrophic lateral sclerosis. *Ann Neurol* 65(Suppl 1):S3–S9.
2. Ilieva H, Polymenidou M, Cleveland DW (2009) Non-cell autonomous toxicity in neurodegenerative disorders: ALS and beyond. *J Cell Biol* 187:761–772.
3. Chattopadhyay M, Valentine JS (2009) Aggregation of copper-zinc superoxide dismutase in familial and sporadic ALS. *Antioxid Redox Signal* 11:1603–1614.
4. McGeer PL, McGeer EG (2002) Inflammatory processes in amyotrophic lateral sclerosis. *Muscle Nerve* 26:459–470.
5. Halle A, et al. (2008) The NALP3 inflammasome is involved in the innate immune response to amyloid-beta. *Nat Immunol* 9:857–865.
6. Pasinelli P, Houseweart MK, Brown RH, Jr, Cleveland DW (2000) Caspase-1 and -3 are sequentially activated in motor neuron death in Cu,Zn superoxide dismutase-mediated familial amyotrophic lateral sclerosis. *Proc Natl Acad Sci USA* 97: 13901–13906.
7. Li M, et al. (2000) Functional role of caspase-1 and caspase-3 in an ALS transgenic mouse model. *Science* 288:335–339.
8. Lamkanfi M, Dixit VM (2009) Inflammasomes: Guardians of cytosolic sanctity. *Immunol Rev* 227:95–105.
9. Urushitani M, et al. (2006) Chromogranin-mediated secretion of mutant superoxide dismutase proteins linked to amyotrophic lateral sclerosis. *Nat Neurosci* 9:108–118.
10. Zhao W, et al. (2010) Extracellular mutant SOD1 induces microglial-mediated motoneuron injury. *Glia* 58:231–243.
11. Hornung V, et al. (2008) Silica crystals and aluminum salts activate the NALP3 inflammasome through phagosomal destabilization. *Nat Immunol* 9:847–856.
12. Levine B, Deretic V (2007) Unveiling the roles of autophagy in innate and adaptive immunity. *Nat Rev Immunol* 7:767–777.
13. Hetz C, et al. (2009) XBP-1 deficiency in the nervous system protects against amyotrophic lateral sclerosis by increasing autophagy. *Genes Dev* 23:2294–2306.
14. Kuma A, et al. (2004) The role of autophagy during the early neonatal starvation period. *Nature* 432:1032–1036.
15. Gurney ME, et al. (1994) Motor neuron degeneration in mice that express a human Cu,Zn superoxide dismutase mutation. *Science* 264:1772–1775.
16. Dinarello CA (2009) Immunological and inflammatory functions of the interleukin-1 family. *Annu Rev Immunol* 27:519–550.
17. Nguyen MD, Julien JP, Rivest S (2001) Induction of proinflammatory molecules in mice with amyotrophic lateral sclerosis: No requirement for proapoptotic interleukin-1beta in neurodegeneration. *Ann Neurol* 50:630–639.
18. Hensley K, et al. (2006) Primary glia expressing the G93A-SOD1 mutation present a neuroinflammatory phenotype and provide a cellular system for studies of glial inflammation. *J Neuroinflammation* 3:2–10.
19. Bruijn LI, et al. (1997) ALS-linked SOD1 mutant G85R mediates damage to astrocytes and promotes rapidly progressive disease with SOD1-containing inclusions. *Neuron* 18:327–338.
20. Rakhit R, et al. (2007) An immunological epitope selective for pathological monomer-misfolded SOD1 in ALS. *Nat Med* 13:754–759.
21. Zetterström P, et al. (2007) Soluble misfolded subfractions of mutant superoxide dismutase-1s are enriched in spinal cords throughout life in murine ALS models. *Proc Natl Acad Sci USA* 104:14157–14162.
22. Prudencio M, Hart PJ, Borchelt DR, Andersen PM (2009) Variation in aggregation propensities among ALS-associated variants of SOD1: Correlation to human disease. *Hum Mol Genet* 18:3217–3226.
23. Stewart CR, et al. (2010) CD36 ligands promote sterile inflammation through assembly of a Toll-like receptor 4 and 6 heterodimer. *Nat Immunol* 11:155–161.
24. Tükel C, et al. (2009) Responses to amyloids of microbial and host origin are mediated through toll-like receptor 2. *Cell Host Microbe* 6:45–53.
25. Friedlander RM (2000) Role of caspase 1 in neurologic disease. *Arch Neurol* 57: 1273–1276.
26. Moisse K, Strong MJ (2006) Innate immunity in amyotrophic lateral sclerosis. *Biochim Biophys Acta* 1762:1083–1093.
27. Hall ED, Oostveen JA, Gurney ME (1998) Relationship of microglial and astrocytic activation to disease onset and progression in a transgenic model of familial ALS. *Glia* 23:249–256.
28. Habisch HJ, et al. (2007) Intrathecal application of neuroectodermally converted stem cells into a mouse model of ALS: Limited intraparenchymal migration and survival narrows therapeutic effects. *J Neural Transm* 114:1395–1406.